PERFORMANCE INVESTIGATION OF THERMAL MANAGEMENT SYSTEM ON BATTERY ENERGY STORAGE CABINET

by

Indra PERMANA[a], Alya Penta AGHARID[b], Fujen WANG[b*], and Shih Huan LIN[c]

[a] Graduate Institute of Precision Manufacturing, National Chin-Yi University of Technology, Taichung, Taiwan
[b] Department of Refrigeration, Air Conditioning, and Energy Engineering, National Chin-Yi University of Technology, Taichung, Taiwan
[c] Green World Electric and Energy Saving Consultant Co. Ltd., Taichung, Taiwan

Original scientific paper
https://doi.org/10.2298/TSCI221227154P

Energy storage like batteries is essential for stabilizing the erratic electricity supply. High temperatures when the power is charged and discharged will produce high temperatures during the charging and discharging of batteries. To maintain optimum battery life and performance, thermal management for battery energy storage must be strictly controlled. This study investigated the battery energy storage cabinet with four cases studies numerically. The results show that Case 1, as the initial design not performing optimally. Thermal buoyancy occurs, resulting in the temperature in the top area being warmer than the lower area. The battery surface temperature is steadily at 47 °C. Case 2 added fans on the center of the cabinet bottom surface to overcome the problem, while Case 3 added fans on the left side of the cabinet bottom surface. The battery surface temperatures in Cases 2 and 3 are steady at 39 °C and 37 °C. However, high temperatures still accumulated in the top area for both cases. Contrarily, Case 4 performs a better thermal distribution by adding exhaust air to the top side of the cabinet. The results revealed that the placement of exhaust air could enhance the removal of heat generated from the batteries accumulated in the top area. The battery surface temperature in Case 4 is relatively at 35 °C. Case 4 also performs the best thermal distribution, which desired temperature could be successfully achieved faster compared to other cases.

Key words: *energy storage, battery cabinet, thermal management, temperature uniformity, numerical simulation*

Introduction

Electrification of the grid is one of the most important applications of battery energy storage systems (BESS). Gradual advancements in energy storage technology result in significant cost reductions and improved system efficiency. As a result, its demand in the market will most likely increase throughout the projection period [1]. It would be ideal for producing useful electrical energy from the battery-stored energy. However, as current passes through the electrodes, losses result from polarization. These losses are brought on by the effects of

* Corresponding author, e-mail: fjwang@ncut.edu.tw

ohmic, activation, and concentration polarization [2]. The impact of ohmic, kinetic polarization, and concentration often diminishes with temperature. Consequently, the battery capacity increases, which is uncommon due to increasing self-discharge [3]. However, rising temperatures have a major impact on both battery life and performance [4]. This underlines how essential it is to achieve the best possible exchange between temperature and polarization effects. To better understand how lithium battery voltage, temperature, and capacity change over time, Wang *et al.* [5] conducted a study examining the availableness and safety of the batteries at several ambient temperatures, current variable rates, and charge-discharge cycles. Under varied working conditions, the voltage plateau properties of lithium batteries are studied. According to the results, when discharging at current rates of 0.1 C, 0.25 C, 0.5 C, 0.75 C, and 1 C in temperatures of 5 °C, 10 °C, 25 °C, and 40 °C. From the study, it is revealed that batteries will increase their temperature during the charge-discharge period.

The temperature has a major impact on how well Li-ion batteries work. Between 20 °C and 50 °C is the ideal operating temperature range for a Li-ion battery [6]. A Li-ion battery ideal operating temperature is between 25 °C and 40 °C [7]. The optimal temperature and uniformity of the battery energy storage must be maintained to cultivate battery stability and extend battery life [8, 9]. In order to prevent safety issues (thermal intensification) and capacity decline associated with temperature beyond the desired temperature range, advanced thermal management systems with precise temperature control are necessary [10]. To increase performance and safety, battery thermal management systems (BTMS) must be effective. It is essential to choose a suitable BTMS based on the function of the battery and mix different approaches to make up for the drawbacks to ensure safety and extended battery life [11, 12].

The BTMS, which can effectively regulate the thermal load on the battery, is essential for ensuring the safety and performance of Li-ion batteries during design. The BTMS, which can effectively control the thermal load on the battery, is necessary for ensuring the safety and performance of Li-ion batteries during design. The most common single-phase cooling option is the air-cooled BTMS because of how simple it is to integrate with other systems [13]. In essence, forced convection is used for cooling. An active air-cooled BTMS uses forced convection as an active air supply method, which requires excessive power from the battery. Maximizing the efficiency of battery packs requires this parasitic power usage optimization [14].

According to [15-17] studies, higher battery location can make air cooling an efficient thermal management drop. It shows that the design of the energy storage could affect the thermal uniformity in the system. The problem discovered by Yang *et al.* [18] and Chen *et al.* [19] identified as being similar is that fins are a useful approach to improving heat exchange by enhancing the heat transfer contact area. In a vertical thermal energy storage unit, there was a strong inconsistent dissolving behavior, including dissolving fraction and temperature uniformity. An experimental and numerical examination of the thermal management of an outdoor battery storage cabinet was conducted by Zhang *et al.* [20] to gauge the battery surface temperatures and verify the accuracy of the numerical calculations, and an experimental facility was created. The results of CFD simulation and experiments differ by 2.1% or 0.54 °C of average battery surface temperature.

This study intends to evaluate the impact of various parameters on the thermal performance of the battery energy storage cabinet to acquire good thermal performance from the design of the battery energy storage cabinet through measurement and simulation with several case studies. From a number of empirical, it is determined which design can remove battery-

generated heat during the charge and discharge phases. In addition, this study explores which design will achieve the battery energy storage cabinet's target temperature more efficiently.

The BESS

The BESS are a bundle of hardware and software that enable energy from renewable sources to be stored and released to provide a consistent electrical supply. These batteries help power grids, and consumers maintain a steady supply of renewable energy. Figure 1 shows how the BESS diagram operates. Initially, RES were used to charge a battery management system (BMS). The power conversion system (PCS) must convert the BMS stored energy. By doing so, the alternating current (AC) required by facilities is generated from the direct current of the batteries (DC). In battery energy storage systems, bidirectional inverters are used to permit charging and discharging. The energy management system (EMS) monitors and manages the energy flow within a battery storage system. A BESS EMS component co-ordinates the activities of the PCS, BMS, and other components. By gathering and examining energy data, it can effectively optimize the power resources of the systems. Depending on its functionality and operational conditions, a BESS may include a smoke detector, fire control system, temperature control system, and HVAC systems. In an energy grid outage, a BESS can provide backup power until the electricity is fully restored. Due to the enhanced storage capacity and integration with renewable energy sources, it could also store energy for extended durations.

Figure 1. Diagram of BESS

Methodology

Experimental set-up and measurement

Figure 2 illustrates the design of the battery energy storage cabinet with a length of 1300 mm, a width of 860 mm, and a height of 2130 mm. The geometry model was created by using SOLIDWORKS. The energy storage consists of the cabinet itself, the battery for energy storage, the BMSS to control the batteries, the panel, and the air conditioning to maintain the battery temperature in optimal condition. The cooling capacity from the AC is 0.45 kW. Each side of the cabinet has 16 batteries, 1 panel, and 1 AC system.

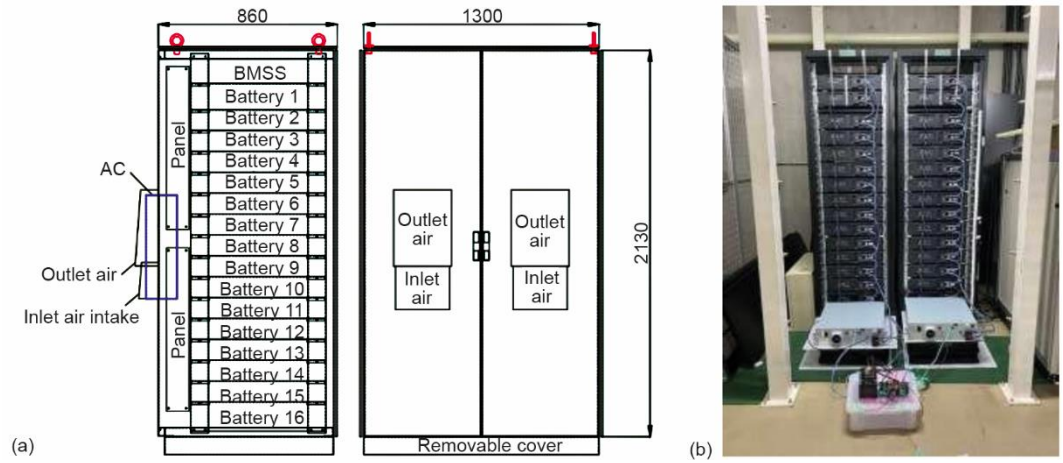

Figure 2. The experimental set-up of battery cabinet; (a) schematic design, and (b) photograph

The CFD simulation

The ANSYS FLUENT 2020 R2 was implemented in this study to numerically simulate the air-flow and temperature distribution on the battery cabinet. Numerous equations are provided by ANSYS FLUENT to resolve issues with laminar and turbulent fluid-flow, incompressible and compressible fluid, and other issues. The ANSYS resolves the mass, momentum, and energy conservation equations to solve the flow and temperature fields of the issue. Most engineering flow field calculations use the standard k-ε turbulence model, which simulates steady-state turbulence in three dimensions, and the continuity equation is solved using the finite volume method (FVM). This method solves a system of equations including the continuity equation, momentum equation, energy equation, turbulence kinetic energy, and dissipation rate transfer:

$$\frac{\partial}{\partial t}(\rho\phi) + \nabla(\rho\vec{\mathrm{V}}\phi - \Gamma_{\phi,\mathrm{eff}}\nabla\phi) = S_\phi \tag{1}$$

where ρ is the fluid density, ϕ – the variable of the different transfer equation, and $\vec{\mathrm{V}}$ – the velocity vector. The parameters ϕ, $\Gamma_{\phi,\mathrm{eff}}$, and S_ϕ describe a continuous equation, momentum equation, and energy equation as follows.

Continuity equation

Let $\phi = \mu_t$, $\Gamma_{\phi,\mathrm{eff}} = 0$, and $S_\phi = 0$ be substituted into eq. (1), which can derive:

$$\frac{\partial\rho}{\partial t} + \frac{\partial}{\partial x_t}(\rho\mu_t) = 0 \tag{2}$$

Momentum equation

Let $\phi = 1$, $\Gamma_{\phi,\mathrm{eff}} = \mu_e$, and $S_\phi = (-\partial\rho/\partial x_i) + F_1$ be substituted into eq. (1), which can derive:

$$\frac{\partial}{\partial t}(\rho\mu_i) + \frac{\partial}{\partial x_j}(\rho\mu_j\mu_i) = -\frac{\partial p}{\partial x_i} + \frac{\partial}{\partial x_j}\left(u_e\frac{\partial\mu_t}{\partial x_j}\right) + F_i \tag{3}$$

where the $\mu_e = \mu + \mu_i$ of eq. (3) is the sum of the laminar flow and the turbulent viscous coefficient, *i.e.*, the effective viscosity coefficient and F – the external body forces in the i direction or the other user-defined source items such as porous media.

Energy equation

Let $\phi = T$, $\Gamma_{\phi,\text{eff}} = k_e$, and $S_\phi = S_e$ be substituted into eq. (1), which can derive:

$$\frac{\partial}{\partial t}(\rho c_p T) + \frac{\partial}{\partial x_j}(\rho c_p T \mu_i) = -p\frac{\partial u_i}{\partial x_i} + \frac{\partial}{\partial x_j}\left(k_e \frac{\partial T}{\partial x_j}\right) + \mu\phi + S_e \tag{4}$$

This study conducted three improvement designs, illustrated in fig. 3. The improvements were expected to enhance the thermal performance in the original design, which simultaneously improves the operation of the battery energy storage. Various improvement designs are described below.

– Case 1: the original design, fig. 3(a).
– Case 2: improvement by adding fans on the bottom mid area, fig. 3(b).
– Case 3: improvement by adding fans on the bottom side area, fig. 3(c).
– Case 4: improvement by adding fans on the bottom mid area and exhaust air on the top area, fig. 3(d).

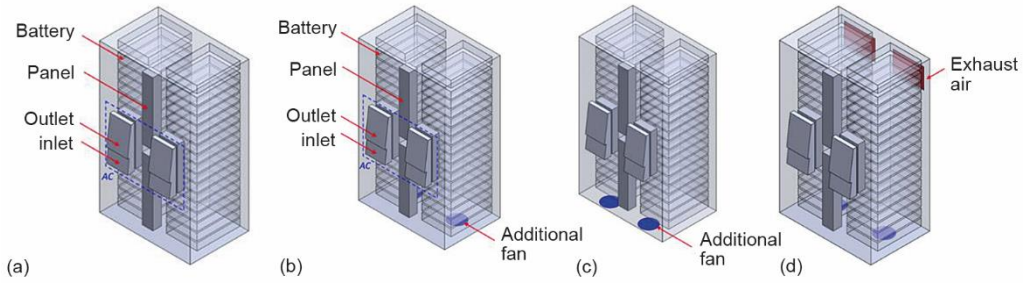

Figure 3. The geometry model of the battery cabinet; (a) Case 1, (b) Case 2, (c) Case 3, and (d) Case 4

Based on the results of the experimental observations, the boundary condition for the numerical simulation was established. With an ambient temperature of 22 °C for each example, tab. 1 indicates the parameter and boundary conditions for simulation. The battery cabinet AC produces a supply air of 2.5 m/s and 20 °C in temperature. Each battery pack produces a heat flux of 8.72 W/m^2 [20]. In this simulation, all battery surfaces were assumed to have uni-

Table 1. The boundary condition for the simulation

Parameters	Type	Value
Inlet air	Velocity inlet	Velocity: 2.5 m/s Temperature: 20 °C
Outlet air	Pressure outlet	Temperature: 27 °C
Battery	Heat flux	1 Battery: 8.72 W/m^2 [20] 32 Batteries: 279.04 W/m^2
BMSS	Heat flux	9.88 W/m^2
Additional fan, Delta PFB1224EHEV14	Velocity inlet	Velocity: 6.96 m/s

form heat fluxes for simplification. All wall borders were modeled using the no-slip boundary condition in the radiative heat transfer calculations. The iterative coupling calculation for this stage is solved using the SIMPLE with a total simulation time of 5000 iterations. The air-flow and temperature distribution were evaluated and examined using the steady-state simulation. The numerical simulation was run until the residuals of velocity, and continuity were below 10^{-4}, and the residuals for energy were below 10^{-6} to produce more accurate results.

Result and discussion

Experimental results during charging and discharging

The experimental measurement for the battery energy storage cabinet took approximately 4 hours to charge, fig. 4(a), and 2.5 hours to discharge, fig. 4(b). Voltage, current, and temperature were the three variables that were measured during this experiment. Voltage [V] is shown on the yellow line, current [A] is shown on the blue line, and temperature [°C] is shown on the orange line. The temperature inside the battery energy storage cabinet began at 22 °C and rose gradually over 4 hours, reaching a peak of about 40 °C. The string voltage rose from 750 V to 910 V, and the current remained constant at around 30 A. The temperature was the same, starting at 22 °C, as during the discharge period. However, the temperature rises to 45 °C and remains stable after 2.5 hours. Additionally, the current is greater than the charging period's average of 60 A. The voltage then dropped due to drawing energy from the battery energy storage cabinet or supplying it. Finally, the findings showed that the discharging time might have a greater temperature and a faster time to reach. In light of the experimental results, we assess the battery energy storage cabinet using numerical simulation throughout the discharge time and several design strategies to enhance its thermal performance.

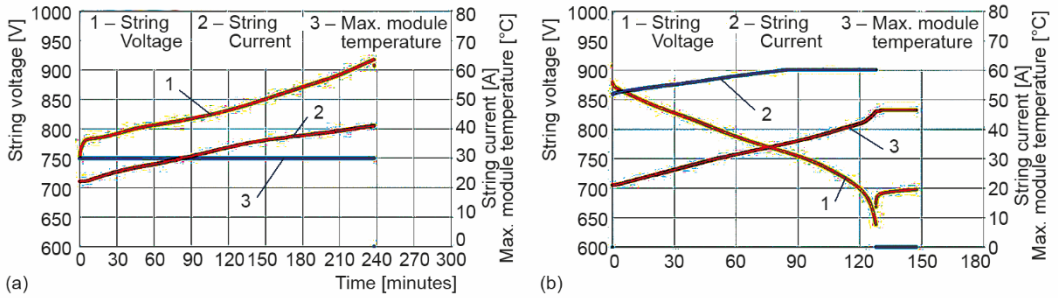

Figure 4. Measurement of battery energy storage cabinet during charging and discharging; (a) charging condition and (b) discharging condition

Grid test and validation

Due to the maximum thermal performance that was measured in the field, the numerical simulation was performed on the current design when discharging the energy. Validation requires error estimation, and uncertainty on both the modeling and measurement sides is required. The experimental measurements are just asserted to be the most accurate representations of reality for validation in this procedure, not that they are more accurate than the modeling results. The validation was also carried out using a different grid number, and the results of the measurements were compared. A polyhedral mesh was implemented to discretize the computing domain. In this work, three alternative mesh element counts were produced and

examined. This study used three different numbers of mesh elements for the grid independence test: coarse grids (1.032.510), medium grids (1.675.220), and fine grids (2.239.710). Equation (5) can be utilized to obtain the error rate [%]:

$$\text{Error rate}\,[\%] = \left|\frac{\text{Measurement} - \text{Simulation}}{\text{Measurement}}\right| 100\% \tag{5}$$

As shown in tab. 2 and fig. 5, finer meshes present a lower error rate than others. Futhermore, the fine mesh was selected for the numerical simulation because they have more precise flow field results and temperature distributions surrounding the batteries.

Table 2. Validation and error rate.

Measurement point	Measurement temperature [°C]	The CFD simulation temperature [°C] and error rate [%]					
		Coarse mesh	Error rate	Medium mesh	Error rate	Fine mesh	Error rate
Point 1	31.10	31.80	2.25	31.35	0.80	31.30	0.64
Point 2	31.50	32.50	3.17	32.05	1.75	31.80	0.95
Point 3	22.60	23.05	1.99	22.85	1.11	22.80	0.88
Point 4	29.50	30.14	2.17	29.65	0.51	29.60	0.34
Point 5	29.00	29.78	2.69	29.15	0. 52	29.12	0.41

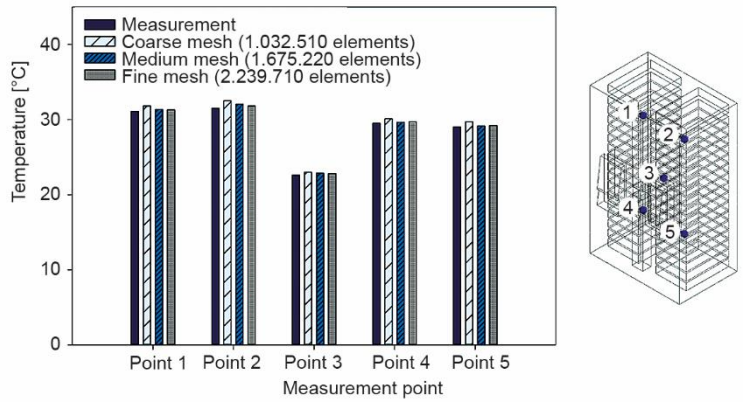

Figure 5. Validation between the field measurement and simulation

Simulation results on existing design during discharging

The result of the thermal performance air-flow velocity in the original battery energy storage cabinet is depicted in fig. 6. In most planes, the air temperature in the cabinet varies from 24 °C to 30 °C. While in Plane 2, the temperature ranges from 20 °C to 26 °C because there is no heat to absorb. But the battery surface temperature in the original design is not uniform, as seen in Planes 1 and 3. The non-uniform heat accumulated on each side battery. It could affect the battery life and performance. The highest temperature in spaces between batteries could be more than 40 °C. Even if the air-flow rate from the AC is set at 2.50 m/s, it is revealed that the air-flow velocity between the batteries decelerates to below 0.40 m/s in the

original design air-flow distribution findings. This prevented the distribution of cool air from the AC to all areas, particularly between the battery spaces, where heat accumulates most during the charge and discharge phases of the energy and batteries.

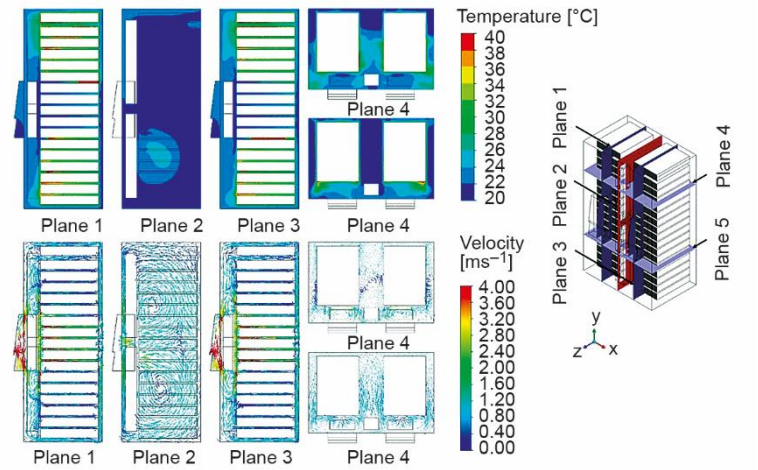

Figure 6. The results of temperature and air-flow velocity distribution in Case 1

Simulation results on improvement design

Improvement strategy by adding fans

The results of the temperature distribution in the improved designs by adding fans are presented in fig. 7. Temperature contour conducts the temperature uniformity in the battery energy storage cabinet in the improved designs by adding fans. From the results, the temperature ranges from 22 °C to 24 °C for the space between the batteries in Case 2. But the temperature increases on the surface of the batteries. The temperature is around 38-40 °C. Case 2 findings are identical to Case 1 because the air-flow from the second fan is obstructed by the batteries, causing the heat generated by the batteries to accumulate in the cabinet's upper and center regions. Therefore, the air-flow distribution in Case 2 did not perform well. The results show that the temperature distribution in Case 3 is also quite similar to Case 2 because the heat still accumulated in the top area of the cabinet. However, the air temperature in Case 3 is slightly warmer than in Case 2. The air temperature is ranged from 26 °C to 30 °C. Although, the battery surface temperature in Case 3 is similar to the Case 2, 38-40 °C. For the temperature uniformity in this plane, Case 3 is better than Case 2. But overall, both improvements are better than the original design.

Improvement strategy by adding fans and exhaust air

Case 4 results in a uniform temperature distribution since the additional fans redistribute the air-flow. It is drawn out by the pressure outlet of the added exhaust air at the top of the cabinet, where the most heat has accumulated. The velocity began at 2.50 m/s at the AC inlet, then decreased to less than 0.40 m/s in the interspaces. At the top region near the exhaust air, it increased to 1.80 m/s. Consequently, the improvement by adding exhaust air resulted in better thermal performance than the other designs, with the temperature surrounding

the cabinet being relatively uniform at 20-24 °C and the range of battery surface temperature is only 28-30 °C.

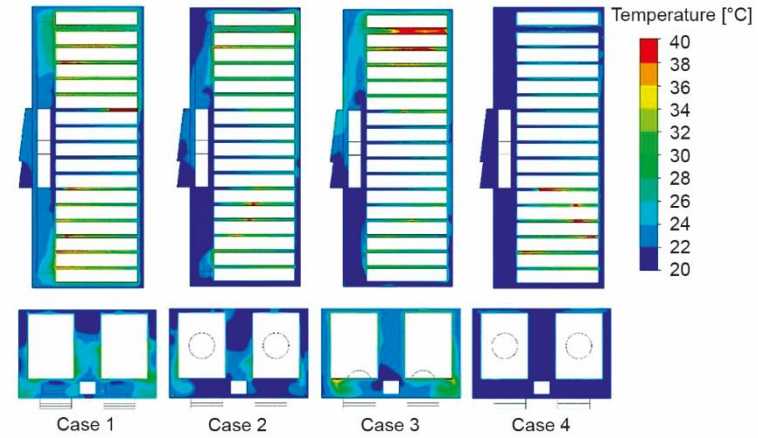

Figure 7. The results of temperature distribution by adding fans

Precisely, measurement points are located in specified positions in the cabinet to identify the temperature uniformity in the systems of each design. Table 3 indicates the measured temperature of each point where thermal performance in Case 4 is relatively uniform. While the minimum temperature at Point 3 is 20.25 °C, and the maximum temperature at Point 5 is 24.15 °C, with an average temperature of 22.57 °C. Compared to other cases, in Case 1, in the original design, the maximum temperature is 32.05 °C, and the minimum temperature is 22.85 °C. With the wide temperature range in Case 1, the average temperature is quite high at 29.01 °C. For Cases 2 and 3, the maximum temperatures are at Point 4, 28.45 °C, and 30.96 °C. The minimum temperatures are quite similar, 21.35 °C at Point 3 in Case 2 and 21.85 °C at Point 3 in Case 3. Hence, the average temperature for Case 2 is 26.09 °C, and for Case 3 is 27.13 °C.

Table 3. The average temperature in each case

Temperature [°C]	Case 1	Case 2	Case 3	Case 4
Point 1	31.35	27.95	27.65	21.95
Point 2	32.05	27.05	28.75	22.45
Point 3	22.85	21.35	21.85	20.25
Point 4	29.65	28.45	30.96	24.05
Point 5	29.15	25.65	26.45	24.15
Average	29.01	26.09	27.13	22.57

Figure 8 shows the temperature performance of each case and measurement result in 150 minutes of operation. It is reported that Case 1 is similar to the measurement result. Temperature becomes steady at around 47 °C after 120 minutes of the system has been operated. After 115 minutes of operation, the temperature stabilizes at approximately 39 °C for Case 2 and 37 °C for Case 3 in the remaining cases. Meanwhile, in Case 4, the temperature becomes

steady at 35 °C after the system is operating for 90 minutes. It indicates that adding a fan to the system can enhance the temperature distribution where the air-flow is redistributed. Furthermore, adding exhaust air could assist the air-flow in circulating to the desired area where the heat mostly accumulated in a shorter time. Therefore, temperature uniformity could be achieved to preserve the battery energy storage cabinet performance.

Figure 8 shows the temperature performance of each case and measurement result in 150 minutes of operation. It is reported that Case 1 is similar to the measurement result. Temperature becomes steady at around 47 °C after 120 minutes of the system has been operated. After 115 minutes of operation, the temperature stabilizes at approximately 39 °C for Case 2 and 37 °C for Case 3 in the remaining cases. Meanwhile, in Case 4, the temperature becomes steady at 35 °C after the system is operating for 90 minutes. It indicates that adding a fan to the system can enhance the temperature distribution where the air-flow is redistributed. Furthermore, adding exhaust air could assist the air-flow in circulating to the desired area where the heat mostly accumulated in a shorter time. Therefore, temperature uniformity could be achieved to preserve the battery energy storage cabinet performance.

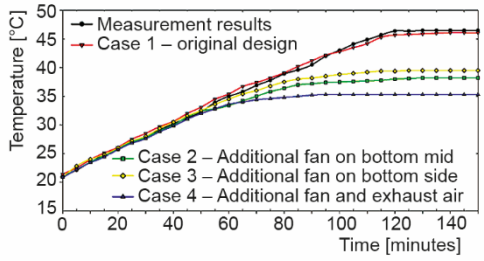

Figure 8. Battery temperature surface results of each case study

The comparison results of thermal performance in each case are illustrated in fig. 9. The comparison results are used to investigate which case could be the best design to implement. In the original design in Case 1, the temperature surrounding the battery module reaches 30-32 °C. Still, the heat accumulated in the top and central areas of the cabinet. In contrast, the temperature of the system is approximately 20 °C to 28 °C cooler in Cases 2 and 3 due to the addition of additional fans. However, heat still accumulated in the top area. Contrarily, in Case 4, adding exhaust air resulted in a better thermal performance than the other designs, with the temperature surrounding the cabinet being relatively uniform at 20-24 °C.

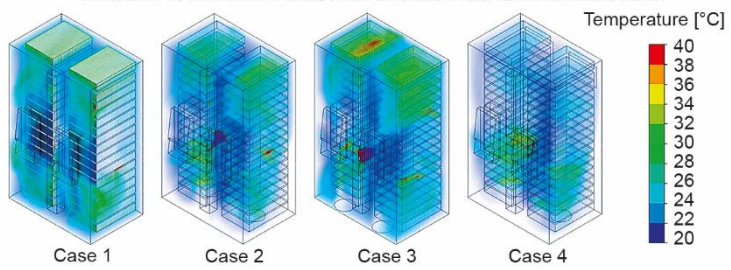

Figure 9. The comparison results of the temperature profile of each case

Conclusion

The design of the battery cabinet storage is one of the factors that cause the flow collision. Air-flow direction, the module structure, and the spacing between cells affect the temperature distribution, which causes temperature non-uniformity in the system. Adding fans in the bottom of the cabinet could maintain the battery surface temperature steadily to 39 °C af-

ter the system operated for 115 minutes. Adding fans at the bottom near the side of the cabinet could maintain the temperature at 37 °C for approximately 115 minutes. While adding fans to the bottom of the cabinet and also adding exhaust air to the top area of the cabinet could enhance thermal performance, with the temperature becoming steady at 35 °C after the system is operating for 90 minutes. Exhaust air could significantly reduce the heat accumulated in a battery energy storage system. Redistributing the air-flow in the system would make it easier to maintain a steady and desirable air temperature. It is possible to achieve the desired temperature uniformity, intending for the best battery energy operation.

Acknowledgment

The Ministry of Science and Technology supported this study under grant no. MOST 109-2622-E-167-002-CC3.

References

[1] Roser, M., *Why did Renewables Become so Cheap so Fast, OurWorldInData.org*., University of Oxford, London, UK, 2020, https://ourworldindata.org/cheap-renewables-growth
[2] Fuller, T. F., Harb, J. N., *Electrochemical Engineering*, John Wiley and Sons Inc., New York, USA, 2018
[3] Linden, D., Reddy, T. B., *Handbook of Batteries*, Mcgraw-Hill, New York, USA, 1995
[4] Feng, H., Song, D., A Health Indicator Extraction Based on Surface Temperature for Lithium-Ion Batteries Remaining Useful Life Prediction, *Journal of Energy Storage, 34* (2021), Feb., 102118
[5] Wang, X., *et al.*, Influence of Different Ambient Temperatures on the Discharge Performance of Square Ternary Lithium-Ion Batteries, *Energies, 15* (2022), 15, 5348
[6] Lv, S., *et al.*, The Influence of Temperature on the Capacity of Lithium Ion Batteries with Different Anodes, *Energies, 15* (2021), 1, 60
[7] Du, W., Chen, S., Effect of Mechanical Vibration on Phase Change Material Based Thermal Management Module of a Lithium-Ion Battery at High Ambient Temperature, *Journal of Energy Storage, 59* (2023), Mar., 106465
[8] Wang, X., *et al.*, A Review of the Power Battery Thermal Management System with Different Cooling, Heating and Coupling System, *Energies, 15* (2022), 6, 1963
[9] Chang, K., *et al.*, Numerical Study of Fuzzy-PID Dual-Layer Coordinated Control Strategy for High Temperature Uniformity of Space Lithium-Ion Battery Pack Based on Thermoelectric Coolers, *Journal of Energy Storage, 56* (2022), Dec., 105952
[10] Vu, H., Shin, D., Simultaneous Internal Heating for Balanced Temperature and State-of-Charge Distribution in Lithium-Ion Battery Packs, *Journal of Energy Storage, 60* (2023), Apr., 106519
[11] Ghaeminezhad, N., *et al.*, A Review on Lithium-Ion Battery Thermal Management System Techniques: A Control-Oriented Analysis, *Applied Thermal Engineering, 219* (2022), Jan., 119497
[12] Xin, S., *et al.*, Thermal Management Scheme and Optimization of Cylindrical Lithium-Ion Battery Pack Based on Air Cooling and Liquid Cooling, *Applied Thermal Engineering, 224* (2023), Apr., 120100
[13] Yang, C., *et al.*, Structure Optimization of Air Cooling Battery Thermal Management System Based on Lithium-Ion Battery, *Journal of Energy Storage, 59* (2023), Mar., 106538
[14] Sharma, D. K., Prabhakar, A., A Review on Air Cooled and Air Centric Hybrid Thermal Management Techniques for Li-Ion Battery Packs in Electric Vehicles, *Journal of Energy Storage, 41* (2021), Sept., 102885
[15] Gocmen, S., Cetkin, E., Emergence of Elevated Battery Positioning in Air Cooled Battery Packs for Temperature Uniformity in Ultra-Fast Dis/Charging Applications, *Journal of Energy Storage, 45* (2021), Jan., 103516
[16] Hai, T., *et al.*, Three-Dimensional Numerical Study of the Effect of an Air-Cooled System on Thermal Management of a Cylindrical Lithium-Ion Battery Pack with Two Different Arrangements of Battery Cells, *Journal of Power Sources, 550* (2022), Dec., 232117
[17] Hai, T., *et al.*, Effect of Air Inlet and Outlet Cross Sections on the Cooling System of Cylindrical Lithium Battery with Segmental Arrangement Utilized in Electric Vehicles, *Journal of Power Sources, 553* (2023), Jan., 232222

[18] Yang, X., *et al.*, Design of Non-Uniformly Distributed Annular Fins for a Shell-and-Tube Thermal Energy Storage Unit, *Applied Energy, 279* (2020), Dec., 115772
[19] Chen, G., *et al.*, Experimental Study On Phase Change Material Based Thermal Management Design with Adjustable Fins for Lithium-Ion Battery, *Applied Thermal Engineering, 221* (2023), Feb., 119808
[20] Zhang, S. B., *et al.*, Improving the Air-Cooling Performance for Lithium-Ion Battery Packs by Changing the Air Flow Pattern, *Applied Thermal Engineering, 221* (2023), Feb., 119825

Paper submitted: December 27, 2022
Paper revised: March 3, 2023
Paper accepted: March 10, 2023

© 2023 Society of Thermal Engineers of Serbia.
Published by the Vinča Institute of Nuclear Sciences, Belgrade, Serbia.
This is an open access article distributed under the CC BY-NC-ND 4.0 terms and conditions.